Journal of
Statistics and Acturial Research
(JSAR)

MODELING OF NATURAL TURBULENT CONVECTION IN AN ENCLOSURE WITH LOCALIZED HEATING

Josephat Kiplagat Kiprop and Dr. Awuor Kennedy Otieno

Journal of Statistics and Actuarial Research
2518-881X (online)
Vol. 2, Issue 1, No. 2, pp 33-49, 2019
www.iprjb.org

MODELING OF NATURAL TURBULENT CONVECTION IN AN ENCLOSURE WITH LOCALIZED HEATING

[1*]Josephat Kiplagat Kiprop
[1]Post Graduate Student: Kenyatta University
*Corresponding Author's E-mail: joserop56@gmail.com
[2]Dr. Awuor Kennedy Otieno
Lecturer: Department of Mathematics, School of Pure and Applied Sciences, Kenyatta University
*Corresponding Author's E-mail: awuor.kennedy@ku.ac.ke

Abstract

Purpose: The purpose of the study was to model natural turbulent convection in an enclosure with localized heating.

Methodology: The study considered the equations governing a free convection. Precisely, the equations governed a Newtonian fluid that experiences transfer of heat or mass. The governing equations were derived from the conservation principles namely the conservation of mass, the conservation of momentum, and the conservation of energy. These equations were decomposed using the Reynolds decomposition then the decomposed equations were non-dimensionalized and reduced using the Boussinesq assumptions. The k-ε model was employed in the simulation of flow characteristics. Finally, the equations were solved numerically for the flow quantities.

Results: The results were presented in form of isotherms and vector potentials in different sections of the enclosure. The results of the study indicated that the variation of the Rayleigh number affects the flow properties such as the velocity and temperature. Specifically, it was found that the increase in the Rayleigh number results in the increase in the velocity magnitude and a decrease in temperature.

Unique contribution to theory, practice and policy: The determination of flow properties is attained with the change in the dimensions of the enclosure and keeping the aspect ratio constant. Furthermore, the bottom wall is heated while the top wall is cold and the other four walls are adiabatic. It is recommended that and investigation is carried out instances where: one makes use of a difference turbulence model such as the k-ω SST turbulence model and observe the fluid properties one carries out an investigation keeping the Rayleigh number constant and varying the aspect ratio and the dimensions of the enclosure and where investigation of the fluid properties in the enclosure with a heater being introduced at the bottom wall and a window at the top wall.

Keywords: *Natural turbulent convection, Localized Heating.*

1.0 INTRODUCTION

A fluid is defined as a substance that undergoes deformation when an external force is subjected to it. The fluid may be a liquid or a gas. There are two categories of fluid mechanics namely fluid kinematics and fluid dynamics. Fluid kinematics involves the study of forces that are involved in the motion of fluids while fluid dynamics involves the study of states of fluid motion. The flow of fluids can be categorized depending on the properties of the fluid or depending on the properties of the flow (Mebrouk, 2016). With regard to the properties of the fluid, there are ideal and real flows, incompressible and compressible flows. On the other hand, the types of flow depending on properties of flow could be laminar and turbulent flow, steady and unsteady flow, or uniform and non-uniform flow. An ideal fluid flow involves the flow of an ideal fluid whereby there is no resistance encountered in the flow while a real fluid flow occurs for a fluid that is viscous in nature and there is a certain amount of resistance to flow. In a uniform flow, the velocity and other parameters such as the pressure of the fluid do not change from one point to the other while in a non-uniform flow there are changes in the hydrodynamic parameters such as pressure and density from one point to the other as the fluid flows (Li, Luo & Fan, 2017).

In an incompressible fluid flow, there is an assumption that the density of the fluid does not change over the flow path while in a compressible flow the density is a function of temperature and pressures in the flow field. A flow in which the fluid particles follow a smooth path and hence does not interfere with each other is called a laminar flow while a turbulent flow is a flow that is characterized by irregular flow and occurs in the instances that the velocity of the fluid is high. In a turbulent flow, there are whirlpools. A steady flow is one in which the fluid properties such as velocity, pressure, temperature, and density are independent of time while in an unsteady flow the fluid properties are functions of time. Specifically, this study was be based on turbulent flow (Mushtaq, Mustafa, Hayat & Alsaedi, 2018).

The transfer of heat can occur in three ways namely conduction, convection, and radiation. In conduction, the transfer of heat occurs when two objects that have different temperatures come in contact with one another. The flow of heat moves from the object with the higher temperature to the one with a lower temperature. Convection is an efficient way of heat transfer in fluids and occurs as a result of differences in temperatures in varying areas of the fluid. Precisely, convection occurs when cooler fluids occupy the place for the warmer fluid resulting in a continuous circulation of fluids. In radiation, the flow of heat does not depend on the availability of any contact between the objects or fluid for heat to be transferred (Daniel & Daniel, 2015).

This study was mainly based on the study of the transfer of heat through convection. In a natural convection, the occurrence of motion of a fluid result from the gravitational field that occurs due to the differences in density resulting from varying temperatures. Along these lines, there was a buoyant force causing dense fluid parts to move to the lower region while the less dense fluid parts to move upwards. The investigation on the effects of the flow of fluids due to buoyancy is applicable in practical occurrences such as in the process of thermal insulation of buildings, cooling of electronic packages, as well as in passive heat removal systems of a liquid metal nuclear reactor among other engineering applications.

1.2 Statement of the Problem

In the past there have been studies on the modeling of natural turbulent convection flow of fluids in an enclosure. Natural convection has myriad applications in the engineering practice including the thermal insulation of buildings. However, the determination of fluid quantities such as velocity, temperature, pressure, and or density is challenging due to the presence of unknown turbulent correlations in the equations governing turbulent flows. This is attributed to the fact that the terms are nonlinear. Along these lines, there is need for the development of a model that could help in solving for the fluid quantities in a natural convection.

1.3 Objectives of the Study

To model natural turbulent convection in an enclosure with Localized Heating.

1.3.1 Specific Objectives

i. To obtain the velocity of flow in different parts of the enclosure.
ii. To determine the temperature variations in different parts of the enclosure.
iii. To determine the effects of varying the Rayleigh number on the heat transfer.

2.0 LITERATURE REVIEW

Different studies have been carried out on natural convection in enclosures. For instance, Altaç and Uğurlubilek (2016) investigated unsteady natural convection heat transfer in 2D and 3D rectangular enclosures using a numerical method. In the study, the rectangular enclosures are heated and cooled from opposing isothermal walls that are vertical to each other and the other side walls of the rectangular enclosure were assumed to be adiabatic and smooth. Further, the fluid used in the study is air and the flow considered is turbulent. Commercial software called FLUENT 6.3.26 was used in solving 2D and 3D continuity equation in the unsteady state, Reynolds-Average Navier-Stokes (RANS), as well as the averaged energy equation. The standard K-ε, Re-Normalization Group k-ε, Realizable k-ε, Reynolds Stress Model, standard k-ω, and the shear stress transport k- ω models were used. Precisely, the performance of turbulence models on heat transfer rates was investigated for 2D and square enclosures and for 3 dimension rectangular enclosures with the slenderness ratio of 1 and 10 respectively. The assessment of heat transfer rates is done by the surface averaged mean Nusselts numbers over the wall that is hot and empirical power-law correlations are deduced. It is noted that identical Nusselt number prediction up to $Ra=10^{10}$ are derived for 3D laminar and RANS models. There are no accurate predictions for the case of a 2D RANS models when there are large Rayleigh numbers. Further, it is concluded that accurate mean Nusselt numbers are yielded from 3D RANS models.

Khanal and Lei (2015) carried out a numerical investigation of the buoyancy induced a turbulent air flow in an inclined passive wall solar chimney that was attached to a room. k- ε model was employed in modeling the air turbulence in the solar chimney system. The investigation is carried out over the Rayleigh number range of $1.36\times10^{13}\leq 1.36\times10^{16}$ and the angle of inclination is between 0^{o} and 6^{o}. The result in the study by Khanal and Lei (2015) indicates that there is a decrease in the amount of turbulent kinetic energy and turbulent intensity in the solar chimney with the increase in the angle of inclination.

Sajjadi and Kefayati (2015) undertook a Lattice Boltzmann simulation of turbulent natural convection with large eddy simulations in tall enclosures that are filled with air (Pr=0.71). High Rayleigh numbers ranging from 10^7 and 10^9 and an aspect ratio change between 0.5 and 2 are used in performing the calculations. The authors concluded that the average Nusselt number increases with the augmentation of Rayleigh numbers leading to a declination in the heat transfer in varying aspect ratios.

Zimmermann and Groll (2014) undertook a numerical study on turbulent natural convection that had large eddy simulation. In the study, the acceleration in natural convection is driven by the differences in local densities and the pressure gradient. The increase in temperature gradients is used in determining the temperature distribution in the heated walls. In the numerical model, the study considered the change in density to occur due to change temperature difference. The study made a comparison of the numerical results with the data from an experimental setup. It was noted that the temperature and the velocity showed an asymmetry as a result of the non-Boussinesq effects of the fluid. In the study, a recommendation for the study of an incompressible turbulent model simulation is made.

3.0 METHODOLOGY

The study considered the equations governing a free convection. Precisely, the equations governed a Newtonian fluid that experiences transfer of heat or mass. The governing equations were derived from the conservation principles namely the conservation of mass, the conservation of momentum, and the conservation of energy. These equations were decomposed using the Reynolds decomposition then the decomposed equations were non-dimensionalized and reduced using the Boussinesq assumptions. The k-ε model was employed in the simulation of flow characteristics. Finally, the equations were solved numerically for the flow quantities.

3.1 Model Description

In this project we will carry out a numerical investigation of turbulent natural convection in 3-dimension. The geometry of the problem is as illustrated in Figure 1 below. The heating of the rectangular enclosure is done on the face-wall. The lower part of the wall is heated (painted red) while the upper half is cooled. The Ampofo and Karayiannis (2003) measurements were used because they carried out the experiment under high accuracy. Precisely, the walls of the rectangular enclosure measure 0.75m by 0.75m by 1.5m wide. The cold and the hot parts of the enclosure were isothermal at 323k and 283k respectively. This gives a Rayleigh number of 1.58×10^9. All the boundaries of the rectangular enclosure are rigid, non-permeable, has no slip. The other walls of the enclosure are adiabatic.

Journal of Statistics and Actuarial Research
2518-881X (online)
Vol. 2, Issue 1, No. 2, pp 33-49, 2019
www.iprjb.org

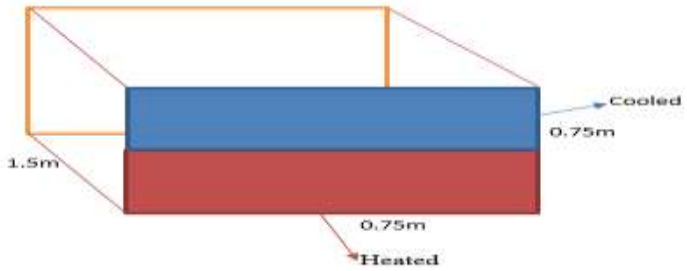

Figure 1: Geometry of the Model

The Boussinesq approximation helped in reducing the governing equations further in this research. In this project, we will zero in on the $k-\varepsilon$ model and the study of variables as used by Ampofo & Karayiannis, 2003).

3.2 Boussinesq Approximation

This is a useful approximation for natural convection or in buoyancy-driven flows in enclosures.

3.3 Simplification of Governing Equations Using Boussinesq Approximation

The variation of density is proportional to temperature and the change is small. This can be shown as follows;

$$\rho = \rho_o + (T+T)\left(\frac{\partial \rho}{\partial T}\right)_{T_o} \tag{4.1}$$

At a constant pressure the coefficient of thermal expansion is given as;

$$\beta_o = \frac{-1}{\rho_o}\left(\frac{\partial \rho}{\partial T}\right)_{T_o} \tag{4.2}$$

On substituting equation (4.2) into equation (4.1) we get;

From (4.1) $\left(\frac{\partial \rho}{\partial T}\right)_{T_o} = \frac{(\rho-\rho_o)}{T-T_o}$ and

From 4.2 $\left(\frac{\partial \rho}{\partial T}\right)_{T_o} = -\rho_o\beta_o$

$$\rho = \rho_o(1-\beta_o(T-T_o)) \tag{4.3}$$

By making use of Boussinesq approximation and equation (4.3) in the governing equations, the presentation of non-dimensional form for an incompressible flow equations that govern natural convection in an enclosure is as follows;

The continuity equation (3.46) becomes;

$$\frac{\partial U_j}{\partial x_j} = 0 \tag{4.4}$$

The momentum equation (3.47) becomes

$$\frac{\partial U_j}{\partial t} + \frac{\partial U_i U_j}{\partial x_j} = \frac{A_1}{\rho_o}\frac{\partial p}{\partial x_i} - A_2\Theta g_i + \frac{\partial}{\partial x_j}\left(A_3\left(\frac{\partial U_i}{\partial x_j} + \frac{\partial U_j}{\partial x_i}\right) - \overline{u_i u_j}\right) \tag{4.5}$$

Where $A_2 = (A_2)_{old}\beta_o \Delta T_*$ and the $(A_2)_{old}$ is given in table (3.1)

The energy equation (3.48) becomes;

$$\frac{\partial \Theta}{\partial t} + \frac{\partial U_j}{\partial x_j}\Theta = \frac{\partial}{\partial x_j}\left(B_2 \frac{\partial \Theta}{\partial x_j} - \overline{u_j \theta}\right) \tag{4.6}$$

The turbulent kinetic energy equation (3.49) simplifies to;

$$\frac{\partial k}{\partial t} + \frac{\partial}{\partial x_j} U_j k = E_1 \overline{u_j \frac{\partial}{\partial x_j} v\left(\frac{\partial u_\iota}{\partial x_j} + \frac{\partial u_j}{\partial x_\iota}\right)} - \frac{\partial}{\partial x_j}\overline{u_j\left(\frac{u_\iota u_j}{2} + \frac{p}{\rho}\right)} - \overline{u_\iota u_j}\frac{\partial U_i}{\partial x_j} + E_2 \overline{\rho u_\iota}\frac{g_i}{\rho}$$

Or

$$\frac{\partial k}{\partial t} + \frac{\partial}{\partial x_j} U_j k = E_1 \overline{u_j \frac{\partial}{\partial x_j} v\left(\frac{\partial u_\iota}{\partial x_j} + \frac{\partial u_j}{\partial x_\iota}\right)} - \frac{\partial}{\partial x_j}\overline{u_j\left(\frac{u_\iota u_j}{2} + \frac{p}{\rho}\right)} - P_k + G_k \tag{4.7}$$

Where

$$P_k = \overline{u_\iota u_j}\frac{\partial U_i}{\partial x_j}\ , G_k = \overline{\rho u_\iota}\frac{g_i}{\rho} \tag{4.8}$$

The specific dissipation equation given by equation (3.50) simplifies to;

$$\frac{\partial \varepsilon}{\partial t} + \frac{\partial}{\partial x_j} U_j \varepsilon = -\frac{\partial}{\partial x_k}\left(F_1 \overline{v u_k \frac{\partial u_\iota}{\partial x_j}\frac{\partial u_k}{\partial x_j}} + F_2 v \overline{\frac{\partial u_k}{\partial x_\iota}\frac{\partial p}{\partial x_\iota}} - F_1 v \frac{\partial \varepsilon}{\partial x_k}\right) - 2F_1 v \overline{\frac{\partial u_\iota}{\partial x_j}\frac{\partial u_\iota}{\partial x_j}\frac{\partial u_k}{\partial x_j}} -$$

$$2F_3\left(\overline{v\frac{\partial^2 u_\iota}{\partial x_k \partial x_j}}\right)^2 + 2F_4 \frac{v}{\rho}\frac{\partial u_i}{\partial x_j}\frac{\partial p}{\partial x_i} g_i - 2F_1 v \frac{\partial u_i}{\partial x_k}\left(\overline{\frac{\partial u_\iota}{\partial x_j}\frac{\partial u_k}{\partial x_j}} + \overline{\frac{\partial u_j}{\partial x_\iota}\frac{\partial u_j}{\partial x_k}}\right) - 2F_1 v \frac{\partial^2 u_i}{\partial x_j \partial x_k} U_k \frac{\partial u_i}{\partial x_j} \tag{4.9}$$

In this case the density is neglected everywhere except in the instance that it causes buoyancy forces. For instance, in equation (4.8) the density is not neglected in G_k because it causes buoyancy forces hence have a contribution to the generation of notation as argued by Gatheri *et al*. (1993).

In these equations the turbulent stress and the heat flux given by $\overline{u_\iota u_j}$ and $\overline{u_j \theta}$ respectively are given by;

$$\overline{u_\iota u_j} = \frac{2}{3}k\delta_{ij} - V_t \tau_{ij}$$

Or

$$\overline{u_\iota u_j} = \frac{2}{3}k\delta_{ij} - v_t\left(\frac{\partial U_i}{\partial x_j} + \frac{\partial U_j}{\partial x_i}\right) \tag{4.10}$$

And

$$\overline{u_j \theta} = -\frac{V_t}{\sigma T}\frac{\partial \Theta}{\partial x_j} \tag{4.11}$$

V_t In equation (4.10) and (4.11) in the $k - \varepsilon$ model is given as

$$V_t = c_\mu \frac{k^2}{\varepsilon} \tag{4.12}$$

3.4 Eliminating the Pressure Term in the Momentum Equation

The primitive variables in the momentum equation (4.5) are the velocity and the pressure. The equation has been written in velocity pressure formulation and has three velocity components and

one pressure component that needs to be solved. The numerical solution of the primitive formulation is possible but there is a challenge in handling the pressure term. For instance, it could bring a challenge in using the same orders of interpolation for both the velocity and pressure. In this project we will use vorticity stream function approach in eliminating the pressure term.

3.4.1 Vorticity Stream function formulation

Equations (4.4) and (4.5) are the non-dimensional forms of the continuity and the momentum equation and may be written in Cartesian coordinate for two dimensional flow to arrive at an accurate formulation of the wall vorticity ξ obtained by Wood (1954) and given as;

$$\xi_b = \frac{3\psi_{b+1}-\psi_b}{(\Delta n)^2} - \frac{1}{2}\xi_{b+1} \tag{4.19}$$

In this equation, b+1 indicates the position that is one mesh point away from the boundary and gives an assumption that there is a linear variation of the vorticity in the interval. However, when this direct approach is used, the boundary conditions will be complicated for one to solve the Navier-stokes equations.

3.4.2 The vector potential formulation for three dimension flow

The vorticity stream function formulation is suited for two dimensional flow problems due to the fact that the stream function does not exist in three dimension and hence it cannot be extended to three dimension. However, a vector potential given as $\psi = \vec{\psi} = \overrightarrow{U_\iota} + \overrightarrow{V_j} + \overrightarrow{W_k}$ exist for solenoidal vector field. Nonetheless, the analogy has not been used much because the equations to be solved does not reduce as expected but instead increase. In addition, the understanding of the boundary conditions is difficult.

In this account, the implementation has only been restricted to the simple cases where the region is closed and connected. As aforementioned the advantage of making use of the vector potential formulation is the there is an automatic satisfaction of the continuity equation. One of the application of vector potential formulation was carried out by Hiroyuki *et al*. (1985) in the study of three dimensional enclosure in which one of the vertical walls was cooled and heated on the floor. In the study, Hiroyuki *et al*. (1985) considered the range of the Rayleigh was 10^6 and 10^7. The vector potential given by ψ is defined as $U = \nabla \times \psi$ and when this is assumed to be solenoidal we will have $\nabla.\psi = 0$. By making use of this definition one can get the velocity components in terms of the stream function as;

$$U = \frac{\partial \psi_3}{\partial y} - \frac{\partial \psi_2}{\partial z}, V = -\left(\frac{\partial \psi_3}{\partial x} - \frac{\partial \psi_1}{\partial z}\right), \; W = \frac{\partial \psi_2}{\partial x} - \frac{\partial \psi_1}{\partial y} \tag{4.20}$$

The relation of vorticity and the stream function is given as;

$$\xi = -\nabla^2\psi \tag{4.21}$$

This can be used in the derivation of the vorticity in three dimension to get the following;

$$\frac{\partial^2\psi_1}{\partial x^2} + \frac{\partial^2\psi_1}{\partial y^2} + \frac{\partial^2\psi_1}{\partial z^2} = -\xi_1, \; \frac{\partial^2\psi_2}{\partial x^2} + \frac{\partial^2\psi_2}{\partial y^2} + \frac{\partial^2\psi_2}{\partial z^2} = -\xi_2, \frac{\partial^2\psi_3}{\partial x^2} + \frac{\partial^2\psi_3}{\partial y^2} + \frac{\partial^2\psi_3}{\partial z^2} = -\xi_1 \tag{4.22}$$

On recasting the momentum equation into a vorticity vector potential one can overcome the problem that is seen in the use of primitive variables, pressure and the need for solving the continuity equation. The three components of the vorticity vector ξ are;

$$\xi_1 = \frac{\partial W}{\partial y} - \frac{\partial V}{\partial z}, \quad \xi_2 = -\left(\frac{\partial W}{\partial x} - \frac{\partial U}{\partial z}\right), \quad \xi_3 = \frac{\partial V}{\partial x} - \frac{\partial U}{\partial y} \tag{4.23}$$

The vorticity transport equation can be obtained by taking the curl of the momentum equation (4.5) as affirmed by Ozoe *et al*. (1976) and hence one will get the transport equation in component form as;

$$\frac{\partial \xi_1}{\partial t} + U\frac{\partial \xi_1}{\partial x} + V\frac{\partial \xi_1}{\partial y} + W\frac{\partial \xi_1}{\partial z} - \xi_1\frac{\partial U}{\partial x} - \xi_2\frac{\partial U}{\partial y} - \xi_3\frac{\partial U}{\partial z} = (A_3 + v_t)\nabla^2\xi_1 + \frac{\partial v_t}{\partial x}\frac{\partial \xi_1}{\partial x} + 2\frac{\partial v_t}{\partial y}\frac{\partial \xi_1}{\partial y} + \frac{\partial v_t}{\partial z}\frac{\partial \xi_1}{\partial z} - \frac{\partial v_t}{\partial y}\frac{\partial \xi_2}{\partial x} - \frac{\partial v_t}{\partial z}\frac{\partial \xi_3}{\partial x} - \left(\frac{\partial^2 v_t}{\partial y^2} + \frac{\partial^2 v_t}{\partial z^2}\right)\xi_1 + \frac{\partial^2 v_t}{\partial x \partial y}\xi_2 + \frac{\partial^2 v_t}{\partial x \partial z}\xi_3 + 2\left[\frac{\partial^2 v_t}{\partial x \partial y}\frac{\partial W}{\partial x} + \frac{\partial^2 v_t}{\partial y^2} + \frac{\partial^2 v_t}{\partial y^2}\frac{\partial W}{\partial y} + \frac{\partial^2 v_t}{\partial y \partial z}\frac{\partial W}{\partial z} - \left(\frac{\partial^2 v_t}{\partial x \partial z}\frac{\partial V}{\partial x} + \frac{\partial^2 v_t}{\partial y \partial x}\frac{\partial V}{\partial y} + \frac{\partial^2 v_t}{\partial z^2}\frac{\partial V}{\partial z}\right)\right] \tag{4.24}$$

$$\frac{\partial \xi_2}{\partial t} + U\frac{\partial \xi_2}{\partial x} + V\frac{\partial \xi_2}{\partial y} + W\frac{\partial \xi_2}{\partial z} - \xi_1\frac{\partial V}{\partial x} - \xi_2\frac{\partial V}{\partial y} - \xi_3\frac{\partial V}{\partial z} = (A_3 + v_t)\nabla^2\xi_2 + 2\frac{\partial v_t}{\partial x}\frac{\partial \xi_2}{\partial x} + \frac{\partial v_t}{\partial y}\frac{\partial \xi_2}{\partial y} + 2\frac{\partial v_t}{\partial z}\frac{\partial \xi_2}{\partial z} - \frac{\partial v_t}{\partial x}\frac{\partial \xi_1}{\partial y} - \frac{\partial v_t}{\partial z}\frac{\partial \xi_3}{\partial y} - \left(\frac{\partial^2 v_t}{\partial x^2} + \frac{\partial^2 v_t}{\partial z^2}\right)\xi_2 + \frac{\partial^2 v_t}{\partial x \partial y}\xi_1 + \frac{\partial^2 v_t}{\partial y \partial z}\xi_3 - A_3\frac{\partial \Theta}{\partial z} + 2\left[\frac{\partial^2 v_t}{\partial x \partial z}\frac{\partial U}{\partial x} + \frac{\partial^2 v_t}{\partial y \partial z}\frac{\partial W}{\partial y} + \frac{\partial^2 v_t}{\partial z^2}\frac{\partial U}{\partial z} - \left(\frac{\partial^2 v_t}{\partial x^2}\frac{\partial W}{\partial x} + \frac{\partial^2 v_t}{\partial x \partial y}\frac{\partial W}{\partial y} + \frac{\partial^2 v_t}{\partial x \partial z}\frac{\partial W}{\partial z}\right)\right] \tag{4.25}$$

$$\frac{\partial \xi_3}{\partial t} + U\frac{\partial \xi_3}{\partial x} + V\frac{\partial \xi_3}{\partial y} + W\frac{\partial \xi_3}{\partial z} - \xi_1\frac{\partial W}{\partial x} - \xi_2\frac{\partial W}{\partial y} - \xi_3\frac{\partial W}{\partial z} = (A_3 + v_t)\nabla^2\xi_3 + 2\frac{\partial v_t}{\partial x}\frac{\partial \xi_3}{\partial x} + 2\frac{\partial v_t}{\partial y}\frac{\partial \xi_3}{\partial y} + \frac{\partial v_t}{\partial z}\frac{\partial \xi_3}{\partial z} - \frac{\partial v_t}{\partial x}\frac{\partial \xi_1}{\partial z} - \frac{\partial v_t}{\partial y}\frac{\partial \xi_2}{\partial z} - \left(\frac{\partial^2 v_t}{\partial x^2} + \frac{\partial^2 v_t}{\partial y^2}\right)\xi_3 + \frac{\partial^2 v_t}{\partial x \partial z}\xi_1 + \frac{\partial^2 v_t}{\partial y \partial z}\xi_2 - A_2\frac{\partial \Theta}{\partial y} + 2\left[\frac{\partial^2 v_t}{\partial x^2}\frac{\partial V}{\partial x} + \frac{\partial^2 v_t}{\partial x \partial y}\frac{\partial V}{\partial y} + \frac{\partial^2 v_t}{\partial x \partial z}\frac{\partial V}{\partial z} - \left(\frac{\partial^2 v_t}{\partial x \partial y}\frac{\partial U}{\partial x} + \frac{\partial^2 v_t}{\partial y^2}\frac{\partial U}{\partial y} + \frac{\partial^2 v_t}{\partial y \partial z}\frac{\partial U}{\partial z}\right)\right] \tag{4.26}$$

The continuity and the momentum equations given by equations (4.4) and (4.5) are replaced by the vorticity transport equations (4.24), (4.25), and (4.26) and equation (4.22).

The variables that are to be solved in this equations are ξ_1,ξ_2 , ξ_3 , U, V, W, Θ , k, and ε. The variables are obtained by solving equations (4.24), (4.25), and (4.26) for ξ_1,ξ_2 , ξ_3 respectively, and U, V, W will be obtained by solving equation (4.20) while k and ε will be obtained by using the turbulent energy equations derived by Ince and Launde (1989) and given as follows;

$$\frac{\partial k}{\partial t} + \frac{\partial}{\partial x_j}U_j k = v_t\left(\frac{\partial U_i}{\partial x_j} + \frac{\partial U_j}{\partial x_i}\right)\frac{\partial U_i}{\partial x_j} - \varepsilon\frac{\partial}{\partial x_j}\left[\left(E_2 + \frac{v_t}{\sigma_k}\right)\frac{\partial k}{\partial x_j}\right] - E_2 g_i\overline{U_\iota\theta} \tag{4.27}$$

$$\frac{\partial \bar{\varepsilon}}{\partial t} + \frac{\partial}{\partial x_j}U_j\bar{\varepsilon} = C_{\varepsilon 1}\frac{\bar{\varepsilon}}{k}v_t\left(\frac{\partial U_i}{\partial x_j} + \frac{\partial U_j}{\partial x_i}\right)\frac{\partial U_i}{\partial x_j} - C_{\varepsilon 2}\frac{\bar{\varepsilon}^2}{k} + 2F_1^2 v_t\left(\frac{\partial^2 U_j}{\partial x_j \partial x_k}\right)^2 + \frac{\partial}{\partial x_j}\left[\left(F_1 + \frac{v_t}{\sigma_\varepsilon}\right)\frac{\partial \bar{\varepsilon}}{\partial x_i}\right] + F_4 g_i\overline{U_\iota\theta}\frac{\bar{\varepsilon}}{k} + 0.83\left(\frac{k^{\frac{3}{2}}}{\bar{\varepsilon}C_1 x_n} - 1\right)^2\frac{\bar{\varepsilon}^2}{k} \tag{4.28}$$

In this equations $\bar{\varepsilon}$ in equation (4.28) is related to the total dissipation ε by the relation;

$$\varepsilon = \bar{\varepsilon} + D \tag{4.29}$$

$D = 2v\left(\frac{\partial k^{\frac{1}{2}}}{\partial x_j}\right)^2$ is the extra rate of destruction in the wall region and far from solid boundary we have $\varepsilon = \bar{\varepsilon}$ because D approaches zero as one goes away from the solid boundary. The empirical coefficient in the study by Launder and Sharma (1974) are given as;

$$C_{\varepsilon 1} = 1.44,\ C_{\varepsilon 2} = 1.92[1 - 0.3exp(-R_t^2)], R_t = \frac{k^2}{F_1 \varepsilon^2}, \sigma_k = 1.0, \sigma_\varepsilon = 1.3 \quad (4.30)$$

3.5 Boundary Conditions

3.5.1 Temperature Boundary Conditions

As defined earlier the non-dimensional temperature was given as $\Theta = \frac{(T - T_*)}{\Delta T_*}$, whereby ΔT_* is the characteristic temperature difference between the cold and the hot surfaces that is $\Delta T_* = T_{hot} - T_{cold}$. The choice of Θ is such that it is bounded between 0 and 1. The isothermal and adiabatic boundary conditions are sued. These conditions are given as

$$\Theta = \text{constant and } \frac{\partial \Theta}{\partial \eta} = 0 \quad (4.31)$$

Respectively where η represents the direction of the wall. Since the problem at hand involves heating on the lower part of the face wall and heating on the upper part of the face wall, the other five walls of the enclosure are kept adiabatic. The Dirichlet boundary conditions are used on the hot part of the wall and the cold part of the wall whereby $\Theta_{hot} = 1$ and $\Theta_{cold} = 0$ are used. On the adiabatic walls, the Neumann boundary condition is used. For each of the adiabatic walls $\frac{\partial \Theta}{\partial \eta} = 0$ is used. For instance, in the x-y plane $\frac{\partial \Theta}{\partial \eta} = 0$.

In the study, the results were obtained for difference Rayleigh numbers and the calculation of the Rayleigh number is carried out as indicated in the formula below;

$$Ra = \frac{g\beta\Delta\rho L^3}{\mu\alpha} = \frac{g\beta\Delta T L^3}{\nu\alpha} \quad (4.32)$$

Where g is the acceleration due to gravity (-9.81)

ρ is the density

μ is the dynamic viscosity

β is the volume of thermal expansively

ΔT the difference in temperature between the hot and the cold walls

ν is the kinematic viscosity,

L is the characteristic length, and

α is the thermal diffusivity

The temperature of the Bottom (hot) wall is kept constant at 313K while the temperature of the top (cold) wall is kept constant at 293K. The aspect ratio is kept constant at 1 and the dimensions of the enclosure are varied for the change in the Rayleigh number. The dimension of the enclosure are 1m by 1 m, 2m by 2m, 4m by 4m, and 18m by 18m to get the Rayleigh numbers of 1.797×10^9, 1.437×10, 1.150×10^{11}, and 1.048×13 respectively. The operating temperature of the enclosure is 303K and the other four walls are kept adiabatic (completely insulated).

3.5.2 Velocity Boundary Conditions

Typically, the conditions in the boundary for a fluid that is in motion depends on the velocity of the fluid. In this case, the boundary conditions that have been used are of no-slip and hence the fluid will have zero velocity in relation to the boundary. In addition, the normal components of velocity at each boundary is zero due to the fact that for a closed cavity the boundary is considered to be impermeable and hence it is capable of motion in its own place only.

3.5.3 Vector Potential Boundary Conditions

In the no-slip boundary, it is difficult to determine the boundary conditions because the components of ψ are not always zero. Only the components that are tangential and those that are normal derivatives are zero. For instance, for the case of the wall along the y-z plane we have $\frac{\partial \psi_1}{\partial x} = 0, \psi_2 = \psi_3 = 0$ at x=0.

Along the x-z plane, $\frac{\partial \psi_2}{\partial y} = 0, \psi_1 = \psi_3 = 0$ at y=0

And along x-y plane, $\frac{\partial \psi_3}{\partial z} = 0, \psi_1 = \psi_2 = 0$ and z=0.

3.5.4 Vorticity Boundary Conditions

The vorticity boundary conditions are obtained from equation (4.21). The vorticity components for the no-slip can be expressed using the fundamental velocities as in equation (4.23). For the wall along y-z, we have $\frac{\partial W}{\partial y} = \frac{\partial V}{\partial z} = \frac{\partial U}{\partial z} = \frac{\partial U}{\partial y} = 0$ using the right hand rule and hence the boundary condition will be given as $\xi_1 = 0, \xi_2 = -\frac{\partial W}{\partial x}, \xi_3 = \frac{\partial V}{\partial x}$.

For the wall along x-y we have $\frac{\partial U}{\partial y} = \frac{\partial V}{\partial x} = \frac{\partial W}{\partial x} = \frac{\partial W}{\partial y} = 0$. this will give the boundary condition as, $\xi_1 = -\frac{\partial V}{\partial z}, \xi_2 = \frac{\partial U}{\partial z}, \xi_3 = 0$

Along x-z wall we have $\frac{\partial W}{\partial x} = \frac{\partial U}{\partial z} = \frac{\partial V}{\partial z} = \frac{\partial V}{\partial x} = 0$. This will give the boundary condition as $\xi_1 = \frac{\partial W}{\partial y}, \xi_2 = 0, \xi_3 = -\frac{\partial U}{\partial y}$

The equations (4.22), (4.23), (4.24), (4.25), (4.26), (4.27), and (4.28) together with the boundary conditions will completely give the mathematical model description for the $k - \varepsilon$ model.

3.6 Numerical Methods

The coupled non-linear differential equations with the boundary conditions are to be solved using the finite difference technique. In this technique, the partial differential equations are to be approximated using a set of linear equations that are related to the values of the functions at specific mesh points and thereafter the set of algebraic equations that are formed are to be solved. The non-linearity of the differential equations necessitate for the development of an iteration procedure and hence calling for the use of the false transient method.

4.0 RESULTS AND DISCUSSION

4.1 Distribution of Streamlines

The path that is traced by a massless particle as it moves with the flow is referred to as the streamline. These are tangent lines to the velocity of flow and are designed to minimize the resistance of flow in the fluid such as air. The results of this study are obtained for Rayleigh numbers ranging from 1.797×10^{9} and 1.048×10^{13}. Figures 6.1 (a), (b), (c), and (d) shows the distribution of streamlines. In figure 6.1 (a), there are two circulating vortices. In this case, a vortex is considered to be a whirling fluid motion. With the increase in the Rayleigh number, it is seen that there is an increase in the number of vortices and stream functions. In addition, the increase in the Rayleigh number causes an increase in the velocity with the maximum velocity in the streamlines for b, c, and d below being $2.51 \times 10^{-1} Kg/s$, $3.50 \times 10^{-1}\, Kg/s$ and, $4.35 \times 10^{-1} Kg/s$ as it can be seen in the figures below. The movement of the streamlines is seen to be from the bottom wall (hot) and down from the top (cold) wall. This observation is in line with the principle of heat transfer. The increase in the Rayleigh number causes an increase in buoyancy forces and hence increase the size of the vortices as well as the strength of the stream function.

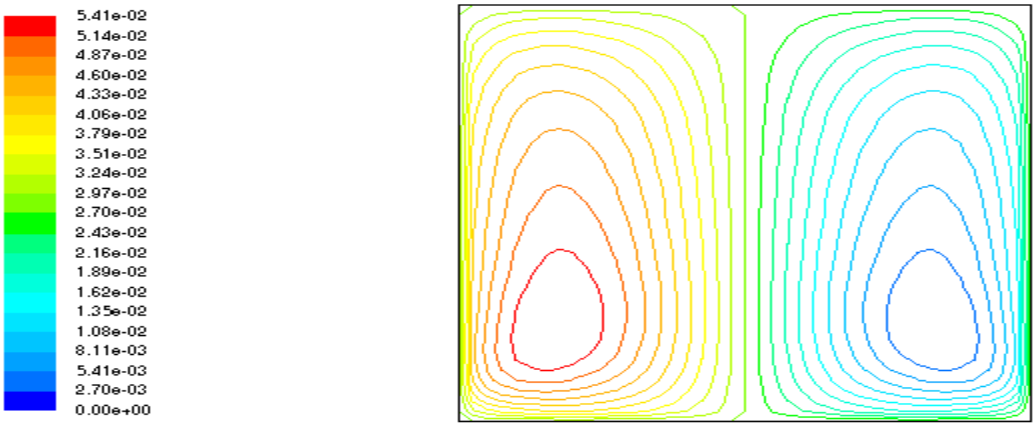

$Ra = 1.797 \times 10^{9}$

$Ra = 1.437 \times 10^{10}$

$Ra = 1.150 \times 10^{11}$

$Ra = 1.048 \times 10^{13}$

Figure 2. Contours of Stream function (Kg/s)

4.2 Contours of Velocity magnitudes

The representation of the contours of velocity magnitudes are shown in Figure 6.2 (a), (b), (c), and (d). With the increase in the Rayleigh number it can be seen that there is an increase in the number of vortices. In addition, the increase in the Rayleigh number results in the increase in the number of streamlines in the bottom (hot) wall. Furthermore, it can be observed that there is an increase in turbulence with the increase in the Rayleigh number because the flow becomes more chaotic with the increase in the Rayleigh number leading to an increase in the velocity magnitude with the minimum velocity magnitude being recorded to be $6.48 \times 10^{-1}\ m/s$ as in figure 6.2 (a) and the maximum velocity being $1.30 \times 10^{0}\ m/s$ in figure 6.2 (a). These is shown in the figures below.

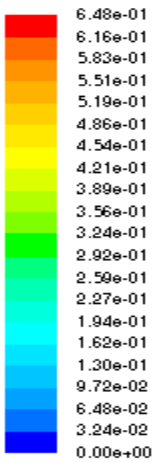

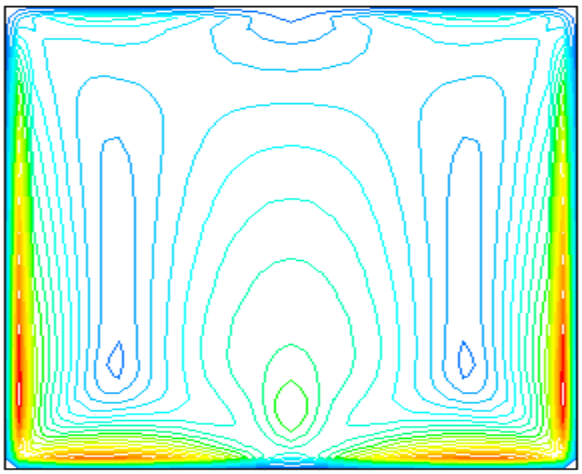

$Ra = 1.797 \times 10^{9}$

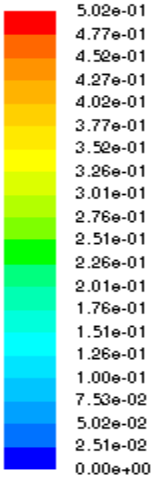

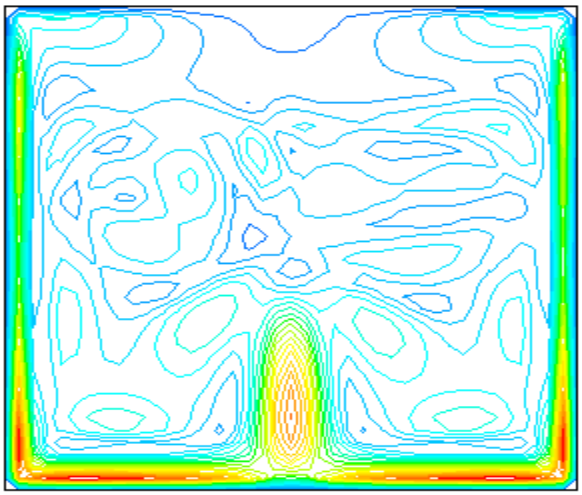

$Ra = 1.437 \times 10^{10}$

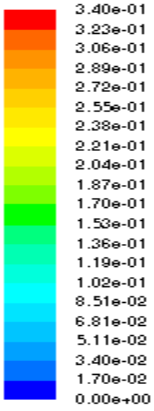

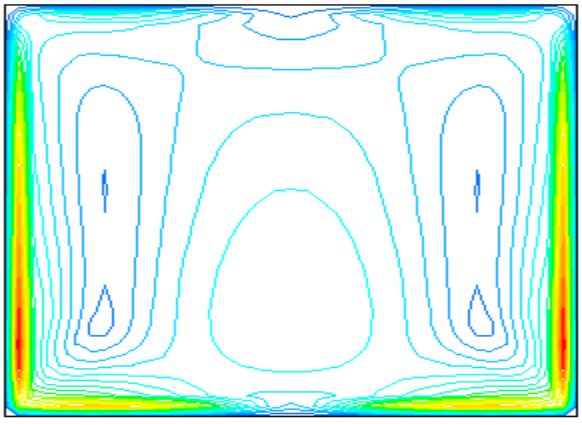

$Ra = 1.150 \times 10^{11}$

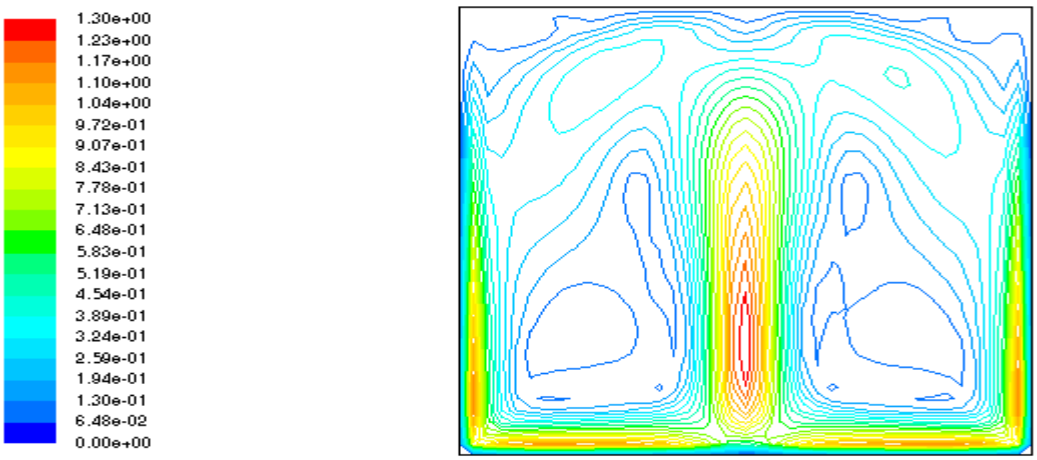

$$Ra = 1.048 \times 10^{13}$$

Figure 3: Contours of Velocity Magnitude (m/s)

4.3 Distribution of Isotherms

An isotherm is a line on a map or a graph connecting parts that have equal temperatures and every given time. Simultaneous temperature readings in different locations help in the creation of isotherms. The contours of the isotherms for difference Rayleigh numbers are represented in the figures 6.3 (a), (b), (c), and (d). The increase in Rayleigh number results in the enlargement and rise of the contours of temperature from the bottom wall with the highest temperature being at the middle part of the face. The temperature with the increase in the Rayleigh number decreases with the maximum temperatures for a, b, c, and d below being indicated as 2.99×10^2 , 2.99×10^2 , 2.96×10^2 , and 2.23×10^2 . Additionally, the number of contours of temperature near the bottom (hot) wall are more and reduce towards the top wall. The transfer of heat through the fluid (air in this case) in the enclosure starts at the bottom wall to the other parts of the enclosure.

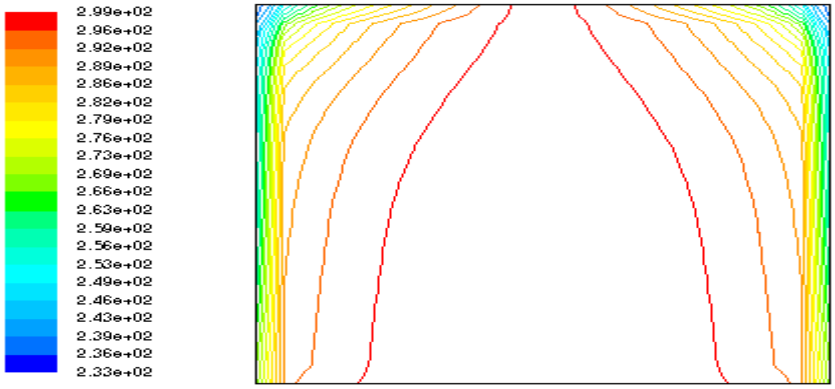

a. $Ra = 1.797 \times 10^9$

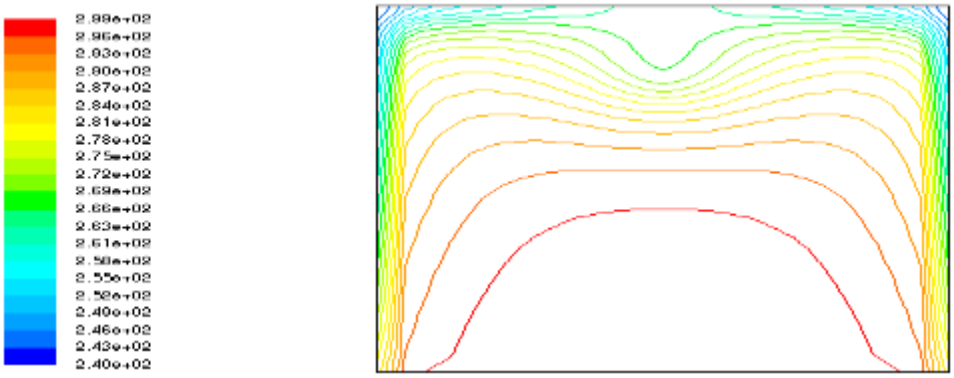

b. $Ra = 1.437 \times 10^{10}$

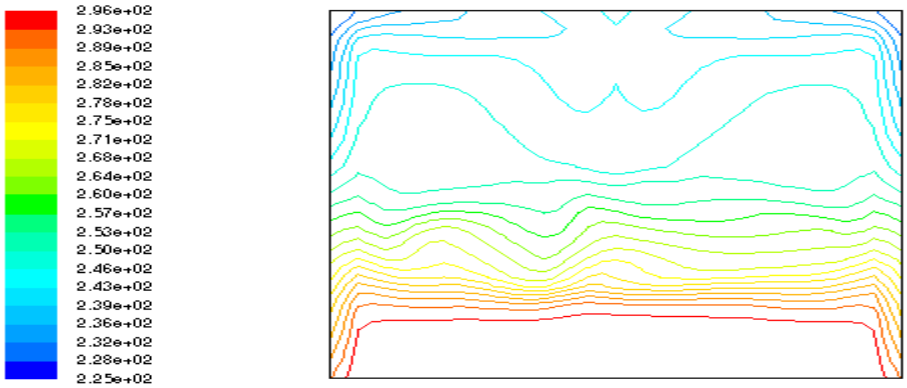

c. $Ra = 1.150 \times 10^{11}$

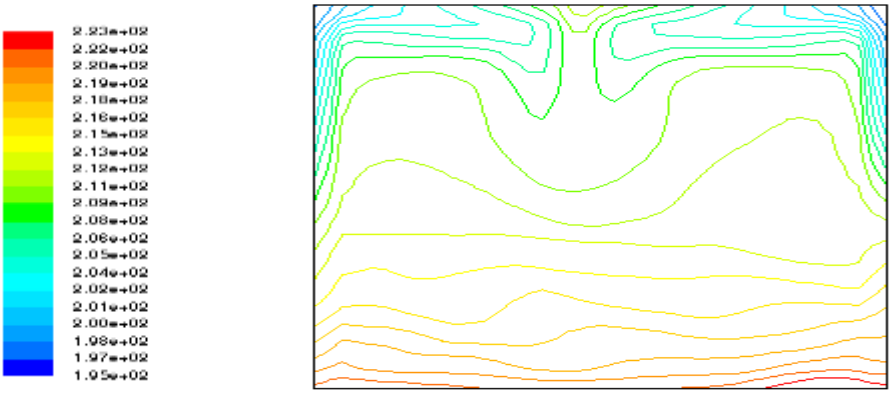

d. $Ra = 1.048 \times 10^{13}$

Figure 4: contours of isotherms (K)

5.0 SUMMARY, CONCLUSIONS AND RECOMMENDATIONS

5.1 Summary

The results are presented in form of isotherms and vector potentials in different sections of the enclosure. The results of the study indicate that the variation of the Rayleigh number affects the flow properties such as the velocity and temperature. Specifically, it is found that the increase in the Rayleigh number results in the increase in the velocity magnitude and a decrease in temperature.

5.2 Conclusions

In this study, the velocity of flow in different parts of the enclosure have been obtained for varying Rayleigh numbers. The results indicate that a variation in the Rayleigh number affects the fluid properties such as velocity and temperature. As such, the velocity magnitude rises with the increase in the Rayleigh number. It is found that an increase in the Rayleigh number results in the increase in the size of vortices. In relation to the temperature distribution in different parts of the enclosure, it is found that the temperature of the enclosure is higher at the bottom of the enclosure and the temperature decreases with the increase in the Rayleigh number. The increase in the Rayleigh number as well is seen to results in an increase in the turbulence and hence the flow becomes more chaotic.

5.3 Recommendations

The determination of flow properties is attained with the change in the dimensions of the enclosure and keeping the aspect ratio constant. Furthermore, the bottom wall is heated while the top wall is cold and the other four walls are adiabatic. It is recommended that and investigation is carried out instances where: one makes use of a difference turbulence model such as the k-ω SST turbulence model and observe the fluid properties one carries out an investigation keeping the Rayleigh number constant and varying the aspect ratio and the dimensions of the enclosure and where investigation of the fluid properties in the enclosure with a heater being introduced at the bottom wall and a window at the top wall.

REFERENCES

Altaç, Z., & Uğurlubilek, N. (2016). Assessment of turbulence models in natural convection from two-and three-dimensional rectangular enclosures. *International Journal of Thermal Sciences*, *107*, 237-246.

Ampofo, F., & Karayiannis, T. G. (2003). Experimental benchmark data for turbulent natural convection in an air filled square cavity. *International Journal of Heat and Mass Transfer*, *46*(19), 3551-3572.

Daniel, Y. S., & Daniel, S. K. (2015). Effects of buoyancy and thermal radiation on MHD flow over a stretching porous sheet using homotopy analysis method. *Alexandria Engineering Journal*, *54*(3), 705-712.

Khanal, R., & Lei, C. (2015). A numerical investigation of buoyancy induced turbulent air flow in an inclined passive wall solar chimney for natural ventilation. *Energy and Buildings*, *93*, 217-226.

Li, D., Luo, K., & Fan, J. (2017). Buoyancy effects in an unstably stratified turbulent boundary layer flow. *Physics of Fluids*, *29*(1), 015104.

Mebrouk, R., Kadja, M., Lachi, M., & Fohanno, S. (2016). Numerical Study Of Natural Turbulent Convection Of Nanofluids In A Tall Cavity Heated From Below. *Thermal Science*, *20*(6).

Mushtaq, A., Mustafa, M., Hayat, T., & Alsaedi, A. (2018). Buoyancy effects in stagnation-point flow of Maxwell fluid utilizing non-Fourier heat flux approach. *PloS one*, *13*(5), e0192685.

Ozoe, H., Yamamoto, K., Churchill, S. W., & Sayama, H. (1976). Three-dimensional, numerical analysis of laminar natural convection in a confined fluid heated from below. *Journal of Heat Transfer*, *98*(2), 202-207.

Sajjadi, H., & Kefayati, R. (2015). Lattice Boltzmann simulation of turbulent natural convection in tall enclosures. *Thermal Science*, *19*(1), 155-166.

Woods, L. C. (1954). A note on the numerical solution of fourth order differential equations. *The Aeronautical Quarterly*, *5*(4), 176-184.

Zimmermann, C., & Groll, R. (2014). Modelling turbulent heat transfer in a natural convection flow. *Journal of Applied Mathematics and Physics*, *2*(07), 662